Interface properties of Pb/InAs planar structures for Andreev spectroscopy

F. Magnus, K. A. Yates, S. K. Clowes, Y. Miyoshi, Y. Bugoslavsky, and L. F. Cohen[a)]
Blackett Laboratory, Imperial College, Prince Consort Road, London SW7 2BZ, United Kingdom

A. Aziz, G. Burnell, and M. G. Blamire
Department of Materials Science and Metallurgy, University of Cambridge, Pembroke Street, Cambridge CB2 3QZ, United Kingdom

P. W. Josephs-Franks
National Physical Laboratory, Teddington TW11 0LW, United Kingdom

(Received 20 September 2007; accepted 6 December 2007; published online 2 January 2008)

For Andreev spectroscopy to be a useful tool to detect spin accumulation in semiconductors, we show by simulation that there is a maximum value for the interface scattering parameter that can be tolerated. Three different fabrication routes for Pb/InAs planar junctions are explored and we find that the "etch-back" processing strategy is the most promising. Using the parameters extracted from the spectroscopic analysis, we find that the interface properties fall into four different regimes of behavior. © *2008 American Institute of Physics*. [DOI: 10.1063/1.2828979]

The development of hybrid metal/semiconductor (N/Sm) spintronic devices requires reliable methods of measuring injected electron spin polarization in semiconductors. In recent years, Andreev reflection[1] (AR) spectroscopy has been widely used to measure the transport spin polarization (P) in magnetic metals[2,3] and magnetic semiconductors.[4,5] It might also be a viable method to detect spin accumulation and diffusion in nonmagnetic metals and semiconductors by making high resolution nanojunction arrays. Indeed, many groups have embraced modern fabrication methods to achieve Andreev nanojunctions.[6,7] However, despite the large body of work on superconductor/semiconductor/superconductor (S/Sm/S) structures,[8,9] fabricating single S/Sm structures with desirable interface properties remains a considerable challenge. Attempts to engineer a transparent S/Sm interface with plasma cleaning have resulted in enhanced effective broadening and suppression of the superconductor energy gap.[10] In addition, high Fermi velocity mismatch contributes[11] to the effective interface scattering barrier strength Z and, as a result, doping of the Sm may be required to reduce the Schottky barrier.[12]

We are interested in developing high resolution Andreev probes[13] to study spin accumulation in narrow gap semiconductors such as InAs and InSb, of interest for spintronics due to their optical properties, high mobility, and high spin-orbit coupling. In the present work, we establish by simulation that there is a maximum workable Z value and we demonstrate that the most feasible route to achieve this is by an "etch-back" processing strategy. Most remarkably, we also find that the interface properties fall into four clearly definable regimes of behavior and we discuss the likely source of these differences.

We compare three routes to process planar structures on 1 μm thick InAs, grown by molecular beam epitaxy.[14] In route 1, a SiO_x mask layer was deposited onto InAs in which apertures were opened using focused ion beam milling (FIB) to define the contact areas. In route 2, apertures were opened in a SiO_x mask layer on InAs using a photolithographic lift-off process. Route 3 involves an etch-back approach where a Pb film (~100 nm thick) was deposited onto InAs before patterning, with the InAs subjected to either (i) a degrease in acetone and isopropanol or (ii) a degrease followed by an 18.5% HCl etch and 2.1% $(NH_4)_2S$ for surface passivation before Pb deposition. Photolithography and Ar^+ ion milling were used to define a mesa structure before backfilling with SiO_x. In all routes, superconducting Pb tracks, crossing the junction areas, were defined using photolithography and lift-off. Routes 1 and 2 are described in more detail elsewhere.[15] The differential conductance of all the junctions was measured four terminally.

The Andreev spectra are analyzed by finding the best least-squares fit to the generalized[16] Blonder-Tinkham-Klapwijk (BTK) theory.[17] There are four fitting parameters: the superconductor energy gap Δ, the spin-polarization P, a generic smearing parameter ω, and the dimensionless effective barrier parameter Z, which has been shown to be a reasonable approximation of the complex underlying physics of the interface.[18] We perform a three parameter fit for a range of fixed P values to obtain the quality of fit function $\chi^2(P)$ and its minimum can be used to predict the correct value of P, as described in more detail in Ref. 19. The smearing parameter ω has also been discussed previously[19] where it was shown that the extracted ω includes the combined effects of thermal and any nonthermal smearing mechanisms without making any assumptions about their origin. For pure thermal broadening, it is defined as $\omega \approx k_B T$.

In order to determine the maximum tolerated Z value for accurate detection of P, we simulate spectra for a range of Z values and show the results of the $\chi^2(P)$ dependence in Fig. 1. The fitting routine cannot find the correct minimum for $Z \geqslant 0.8$ although the correct value of P represents a threshold above which the fit rapidly breaks down. Consequently, the fabrication route must be capable of producing an interface with $Z < 0.8$. The Fermi velocity mismatch between Pb and the InAs surface accumulation layer with a carrier density of $\sim 1 \times 10^{18}$ cm^{-3} results in an effective minimum $Z \sim 0.4$.

Now, let us turn to the experimental exploration of feasibility. Preparation routes 1 and 2 produce a reaction interfacial layer, recognizable by a broad V-shaped conductance background $G_N(V)$, which can be characterized by raising

[a)]Electronic mail: l.cohen@imperial.ac.uk.

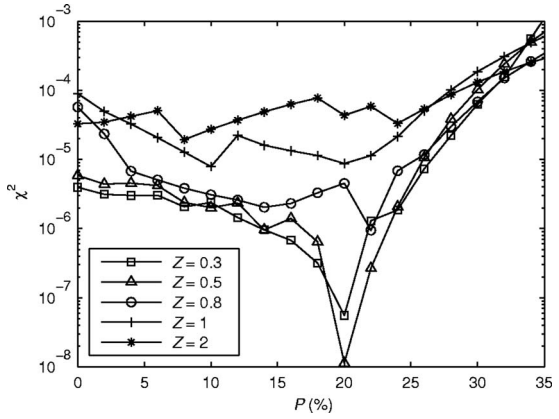

FIG. 1. The $\chi^2(P)$ dependence for simulated spectra with the parameters $\Delta=1$ meV, $\omega=0.3$ meV, $P=0.2$, and varying barrier parameter Z. χ^2 is on a logarithmic scale. The minimum in χ^2 indicates the extracted value of P.

the temperature above the critical temperature of the superconductor T_c or by applying a magnetic field greater than the critical field of the superconductor B_c. In the following, above-T_c normalization will be denoted by $N_{T>Tc}$ and above-B_c normalization with $N_{B>Bc}$. The main graph of Fig. 2 shows a typical conductance spectrum from route 1. The below-T_c and-B_{c2} spectrum shows a dip in conductance around zero bias with barely visible wing peaks, indicative of highly suppressed AR. The presence of a zero bias dip in the above-B_{c2} spectrum confirms that its origin is interfacial and not AR related. Both $N_{T>Tc}$ and $N_{B>Bc}$ yield spectra which can be fitted by BTK theory. The Δ and ω values obtained are similar for both normalization methods but Z is strikingly different. For $N_{T>Tc}$, $Z=3.8$ whereas for $N_{B>Bc}$, $Z=1.9$. In the presence of smearing, Z and P have very similar effects on the shape of the AR spectrum so such a discrepancy in Z will have serious implications for the detection of P.[19] Consequently, we have to explore other routes that do not produce such interfacial layers.

Samples from route 2 share features similar to those of route 1 samples but are almost completely unaffected by the application of $B>B_{c2}$. The temperature dependence of the

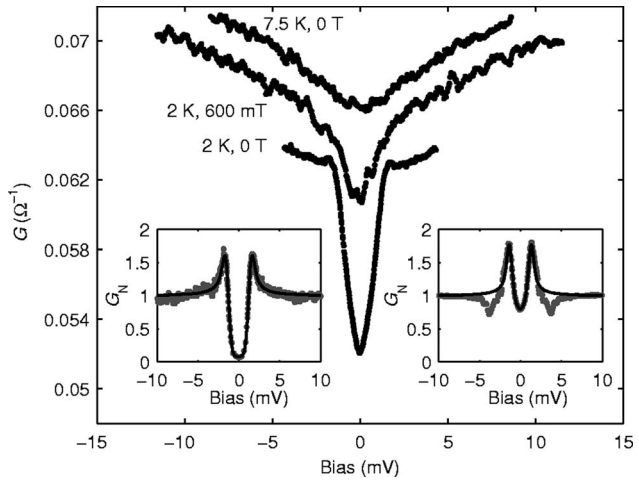

FIG. 2. Main graph: conductance spectra of a route 1 sample below T_c and B_c, above T_c, and above B_c. The above-T_c and above-B_c spectra are offset for clarity. The insets show normalized conductance spectra of route 3(i) sample junctions, illustrating two different types of spectra. The solid black lines are BTK fits. Left inset: $\Delta=1.42$ meV, $Z=2.61$, $\omega=0.22$ meV, and $P=0$. Right inset: $\Delta=1.40$ meV, $Z=0.68$, $\omega=0.16$ meV, and $P=0$.

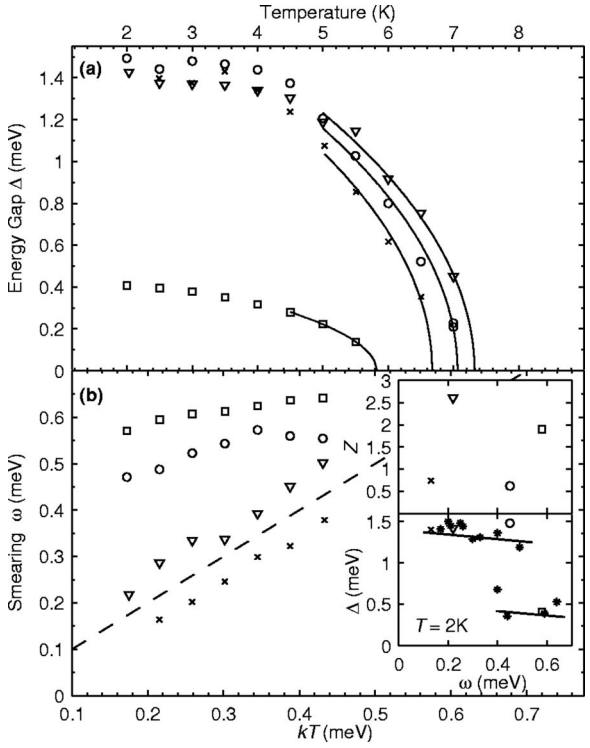

FIG. 3. Temperature dependence of fitting parameters. (a) Superconductor energy gap. Solid lines are fits to the theoretical BCS dependence $(1-T/T_c)^{1/2}$ valid for $T\approx T_c$. (b) Generic smearing parameter. Dashed line represents thermal broadening. Squares: route 1. Circles: route 3(i), low-Z junction. Triangles: route 3(i), high-Z junction. Crosses: route 3(i), low-Z junction. The inset further illustrates the different parameter regimes at 2 K. The symbols refer to the same junctions as in the main graph with additional data denoted by an asterisk. The straight line is a guide to the eye to emphasize the two distinct groups of Δ values. The additional data is omitted in the upper inset for clarity as there is no Z-ω interdependence.

zero bias conductance up to 250 K is well described by tunneling models such as the Stratton model,[20] indicating that route 2 produces tunnel-barrierlike interface properties which dominate over AR. Route 2 does not damage the InAs surface but relies on lift-off of photoresist from the interface, which leaves a chemical residue which strongly affects interface properties.

Route 3 is an etch-back approach where Pb is deposited onto the InAs surface before any processing takes place. The results from route 3(i) samples without the chemical preetch vary significantly due to the roughness, inhomogeneity, and the native In oxide of the InAs surface.[21] The left inset of Fig. 2 shows an example of junctions that show high Z, exceptionally low ω, and a constant $G_N(V)$. This suggests a pinhole-free uniform thin tunnel barrier, and about 25% of junctions show this property. A significant fraction of junctions have a value of Z as low as 0.6 (35% have $Z<1$), very low ω, and a constant $G_N(V)$, as shown in the right inset of Fig. 2. The low-Z junctions also exhibit sharp dip features commonly seen in S/N junctions. Their origin has been widely discussed[22–24] but in our case, they are associated with the superconducting critical current being exceeded in the junction area. Route 3(ii) produces the lowest resistance interfaces, so low in fact that in all but two of the junctions, the Pb/Pb interface (which results from our current processing strategy) dominates the conductance spectrum producing a Josephson junction in series.

Figure 3 shows how the parameters extracted from our

fitting routine suggest distinct regimes of interface properties. Route 1 (using $N_{B>Bc}$) junctions have depressed Δ and high nonthermal broadening. A heavily disordered layer or a very rough interface extending over a depth t greater than the bulk superconducting coherence length ξ would produce inelastic scattering in the superconductor reducing quasiparticle lifetime,[6,25,26] and this is the most likely candidate for these observations. Although an induced proximity layer[6,10] would produce similar observations, this should result from a very clean interface which is unlikely for route 1 junctions. The route 3(i) junctions fall mostly into three other well defined categories, most clearly identified in the inset to Fig. 3. These three categories each have high Δ values but vary in terms of their Z and smearing parameters. Junctions that originate from a rough, disordered layer ($t<\xi$) have high smearing but low Z. Junctions that have a thin homogenous barrier are characterized by high Z but low smearing while the sought after junctions which have a homogenous low scattering barrier show low Z and low smearing. Many of these junctions [including the measurable route 3(ii) junctions] show purely thermal broadening. One of the data sets actually lies below the thermal smearing limit but we can attribute this to the effect of the anomalous conductance dips shown in the inset of Fig. 2 inset. By simulating the effect of exceeding the critical current in the contact region, we find that when the dip voltages are close to the energy gap, they artificially suppress the smearing parameter by up to 30% and this accounts for the observed trend. Apparent broadening less than the thermal limit is, therefore, an artifact of the fitting process if the effects of the conductance dips are ignored. No other data shown in Fig. 3 are affected by this artifact.

Deviation from the thermal smearing line can be attributed to nonthermal smearing effects, which as we discussed earlier can have a variety of origins. We differentiate between behavior where the smearing retains a thermal-like linear temperature dependence but is offset from the purely thermal limit and the more extreme higher residual smearing, which is associated with a much weaker temperature dependence gradient. The latter case either implies that the dominant nonthermal mechanism has an inherently different temperature dependence or that the nonthermal and thermal smearing contributions do not follow a simple sum rule. There is no reason to suppose that they should. However, inelastic scattering is more likely to mimic thermal effects because it spreads the quasiparticle distribution in a similar way and it is plausible that the simple sum rule might apply in this case. This also suggests that the nonthermal smearing in the extreme limit originates from sample inhomogeneity rather than inelastic scattering, but these arguments can only be speculative at this stage.

To summarize, we have established that the interface parameter Z must be below 0.8 for reliable detection of spin polarization using our four parameter model. Exposing the junction to FIB milling or photoresist degrades junction properties severely whereas etch-back processing is capable of producing junctions with a very low interface barrier and negligible nonthermal smearing. We have identified four clear regimes of behavior in our junctions, partly as a result of the different types of processing. Improving reproducibility of junction properties using etch-back methodology with appropriate surface preparation methods and moving to nanojunction arrays is the next task.

This work was supported by the UK Engineering and Physical Sciences Research Council Grants GR/T03802 and EPC511972 and the National Physical Laboratory under the DTI Quantum Metrology Programme.

[1] A. F. Andreev, Zh. Eksp. Teor. Fiz. **46**, 1823 (1964) [Sov. Phys. JETP **19**, 1228 (1964)].
[2] R. J. Soulen, J. M. Byers, M. S. Osofsky, B. Nadgorny, T. Ambrose, S. F. Cheng, P. R. Broussard, C. T. Tanaka, J. Nowak, J. S. Moodera, A. Barry, and J. M. D. Coey, Science **282**, 85 (1998).
[3] S. K. Upadhyay, R. N. Louie, and R. A. Buhrman, Appl. Phys. Lett. **74**, 3881 (1999).
[4] J. G. Braden, J. S. Parker, P. Xiong, S. H. Chun, and N. Samarth, Phys. Rev. Lett. **91**, 056602 (2003).
[5] R. P. Panguluri, K. C. Ku, T. Wojtowicz, X. Liu, J. K. Furdyna, Y. B. Lyanda-Geller, N. Samarth, and B. Nadgorny, Phys. Rev. B **72**, 054510 (2005).
[6] P. Chalsani, S. K. Upadhyay, O. Ozatay, and R. A. Buhrman, Phys. Rev. B **75**, 094417 (2007).
[7] E. Clifford and J. M. D. Coey, Appl. Phys. Lett. **89**, 092506 (2006).
[8] A. W. Kleinsasser, T. N. Jackson, D. McInturff, F. Rammo, G. D. Pettit, and J. M. Woodall, Appl. Phys. Lett. **57**, 1811 (1990).
[9] F. Rahman, T. J. Thornton, R. Huber, L. F. Cohen, W. T. Yuen, and R. A. Stradling, Phys. Rev. B **54**, 14026 (1996).
[10] K. Neurohr, A. A. Golubov, T. Klocke, J. Kaufmann, T. Schapers, J. Appenzeller, D. Uhlisch, A. V. Ustinov, M. Hollfelder, H. Luth, and A. I. Braginski, Phys. Rev. B **54**, 17018 (1996).
[11] I. Zutic and O. T. Valls, Phys. Rev. B **61**, 1555 (2000).
[12] A. Kastalsky, A. W. Kleinsasser, L. H. Greene, R. Bhat, F. P. Milliken, and J. P. Harbison, Phys. Rev. Lett. **67**, 3026 (1991).
[13] F. Magnus, K. A. Yates, B. Morris, Y. Miyoshi, Y. Bugoslavsky, L. F. Cohen, G. Burnell, M. G. Blamire, and P. W. Josephs-Franks, Appl. Phys. Lett. **89**, 262505 (2006).
[14] L. J. Singh, R. A. Oliver, Z. H. Barber, D. A. Eustace, D. W. McComb, S. K. Clowes, A. M. Gilbertson, F. Magnus, W. R. Branford, L. F. Cohen, L. Buckle, P. D. Buckle, and T. Ashley, J. Phys. D **40**, 3190 (2007).
[15] F. Magnus, G. Burnell, Y. Miyoshi, K. A. Yates, Y. Bugoslavsky, S. K. Clowes, P. W. Josephs-Franks, M. G. Blamire, and L. F. Cohen, AIP Conf. Proc. **893**, 1281 (2007).
[16] I. I. Mazin, A. A. Golubov, and B. Nadgorny, J. Appl. Phys. **89**, 7576 (2001).
[17] G. E. Blonder, M. Tinkham, and T. M. Klapwijk, Phys. Rev. B **25**, 4515 (1982).
[18] K. Xia, P. J. Kelly, G. E. W. Bauer, and I. Turek, Phys. Rev. Lett. **89**, 166603 (2002).
[19] Y. Bugoslavsky, Y. Miyoshi, S. K. Clowes, W. R. Branford, M. Lake, I. Brown, A. D. Caplin, and L. F. Cohen, Phys. Rev. B **71**, 104523 (2005).
[20] R. Stratton, J. Phys. Chem. Solids **23**, 1177 (1962).
[21] O. E. Tereshchenko, D. Paget, P. Chiaradia, J. E. Bonnet, F. Wiame, and A. Taleb-Ibrahimi, Appl. Phys. Lett. **82**, 4280 (2003).
[22] L. Shan, H. J. Tao, H. Gao, Z. Z. Li, Z. A. Ren, G. C. Che, and H. H. Wen, Phys. Rev. B **68**, 144510 (2003).
[23] G. Sheet, S. Mukhopadhyay, and P. Raychaudhuri, Phys. Rev. B **69**, 134507 (2004).
[24] G. J. Strijkers, Y. Ji, F. Y. Yang, C. L. Chien, and J. M. Byers, Phys. Rev. B **63**, 104510 (2001).
[25] Y. de Wilde, T. M. Klapwijk, A. G. M. Jansen, J. Heil, and P. Wyder, Physica B **218**, 165 (1996).
[26] R. C. Dynes, V. Narayanamurti, and J. P. Garno, Phys. Rev. Lett. **41**, 1509 (1978).